

WNT signaling pathway regulates *Bmp4* expression in Mesenchymal stromal cells from Acute myeloid leukemia patients

Azevedo, P.L.¹; Oliveira, N. C. A.¹; Corrêa, S.¹; Abdelhay, E.¹; Binato, R.¹

¹Stem Cell Laboratory, Bone Marrow Transplantation Unit, National Cancer Institute (INCA), Rio de Janeiro,

INTRODUCTION

Acute Myeloid Leukemia (AML) is a hematological disease characterized by cellular differentiation arrest, decrease in apoptosis levels, increase in proliferation and accumulation of myeloid precursors in the bone marrow (BM). Although there are several studies in this field, events related to disease initiation and progression remains unknown. The malignant transformation of hematopoietic stem cells (HSC) is thought to generate leukemic stem cells, and this transformation could be related to changes in Mesenchymal stromal cell (hMSC) signaling. A molecular signature from hMSC from AML patients (hMSC-AML) has been proposed by our group, and its gene expression could be related to the leukemic transformation process. We highlight *BMP4*, which has its expression decreased in hMSC-AML and in plasma of AML patients, and this expression could be regulated *in silico* by WNT signaling pathway

Keywords: Acute myeloid leukemia (AML), Mesenchymal stromal cells (MSC), WNT signaling pathway.

OBJECTIVE

In this context, the aim of this work was to verify if WNT signaling is capable of regulating *BMP4* gene in hMSCs

RESULTS

hMSC cultures characterization

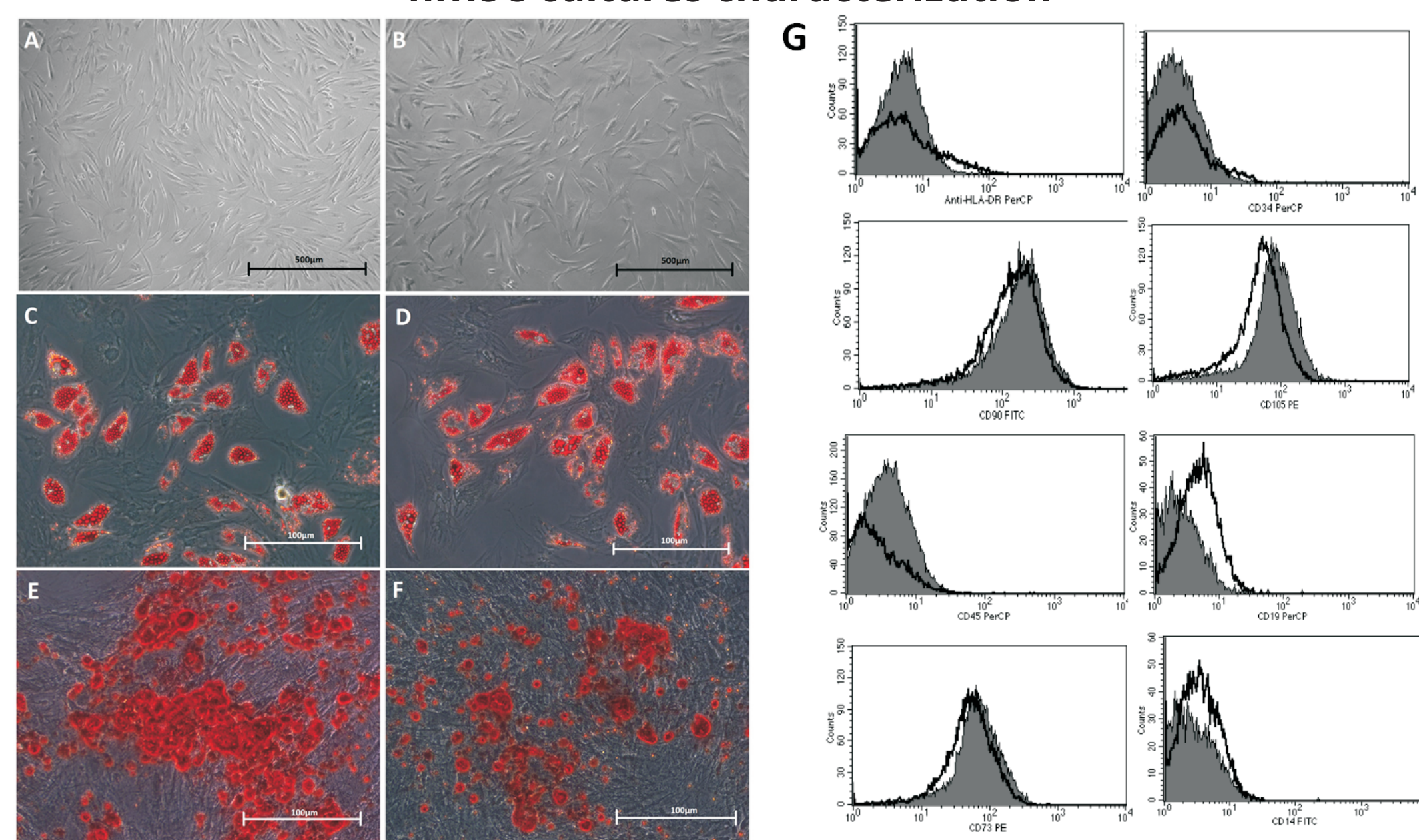


Figure 2: Characterization of hMSC cultures according to ISCT. (A) and (B) – undifferentiated hMSCs from healthy donors (hMSC-HD) and AML patients (hMSC-AML), respectively (200x magnification). (C) and (D) – Adipogenic differentiation from hMSC-HD and hMSC-AML, respectively. Accumulation of neutral lipid vacuoles stained with oil red O indicate differentiation (200x magnification). (E) and (F) – Osteogenic differentiation from hMSC-HD and hMSC-AML, respectively. Calcium deposition stained with alizarin red indicates differentiation (50x magnification). (G) Immunophenotype profile from hMSC-HD and hMSC-AML. The cultures were able to express CD90, CD105, CD73 and CD44, in the absence of lineage commitment markers such as CD45, CD34, CD65 and HLA-DR.

Differentially expressed genes from PCR Array assay

Gene Symbol	Fold Change	Gene Symbol	Fold Change
WNT7B	-23,75	PRICKLE1	1,52
WNT11	-3,40	WNT10A	1,56
WIF1	-2,99	BCL9	1,57
CXXC4	-2,44	FZD3	1,64
TCF7	-2,29	KREMEN1	1,76
PORCN	-2,05	VANGL2	1,85
LEF1	-1,86	FRZB	2,39
WNT16	-1,83	FZD1	2,42
WNT5B	-1,73	MMP7	3,11
PITX2	-1,61	SFRP1	3,20
RHOA	-1,57	FZD9	3,56
TCF7L1	-1,56	SFRP4	3,61
PPARΔ	-1,54	NKD1	9,56

Table 1: List of the 26 differentially expressed genes when compared hMSC-AML and hMSC-HD cultures, identified by PCR Array assay (Human WNT Signaling Pathway). Data were analyzed using GeneGlobal data analysis center (Qiagen) and differentially expressed genes with > ± 1,5 fold-change was used as a criterion to define overexpression or downregulation.

RT-qPCR Confirmation

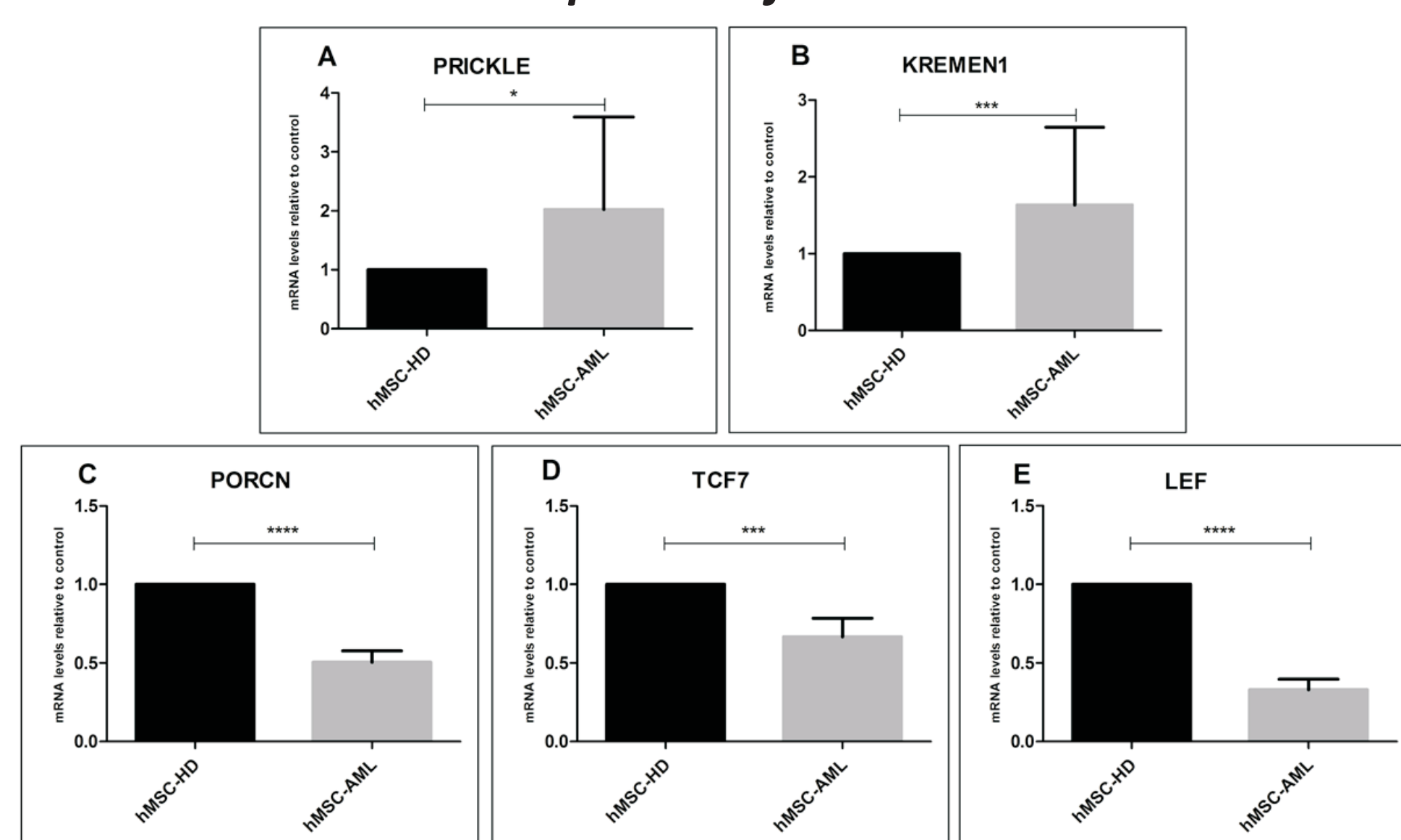


Figure 3: RT-qPCR to validate the PCR array results. To confirm the PCR array results we used RT-qPCR assays to determine changes in mRNA expression of some differentially expressed genes using 30 samples obtained from hMSC-AML and 19 samples obtained from hMSC-HD. Data normalization was performed using the endogenous genes *B2M* and *GAPDH*. The RT-qPCR analyses of *PRICKLE* (A) and *KREMEN1* (B) (overexpressed in hMSC-AML) and *PORCN* (C), *LEF1* (D) and *TCF7* (E) (downregulated in hMSC-AML) confirmed the PCR array results. The bars indicate the means at mRNA levels (± standard deviation) * p < 0.05 / ** p < 0.01 / *** p < 0.001 / **** p < 0.0001.

In silico analysis

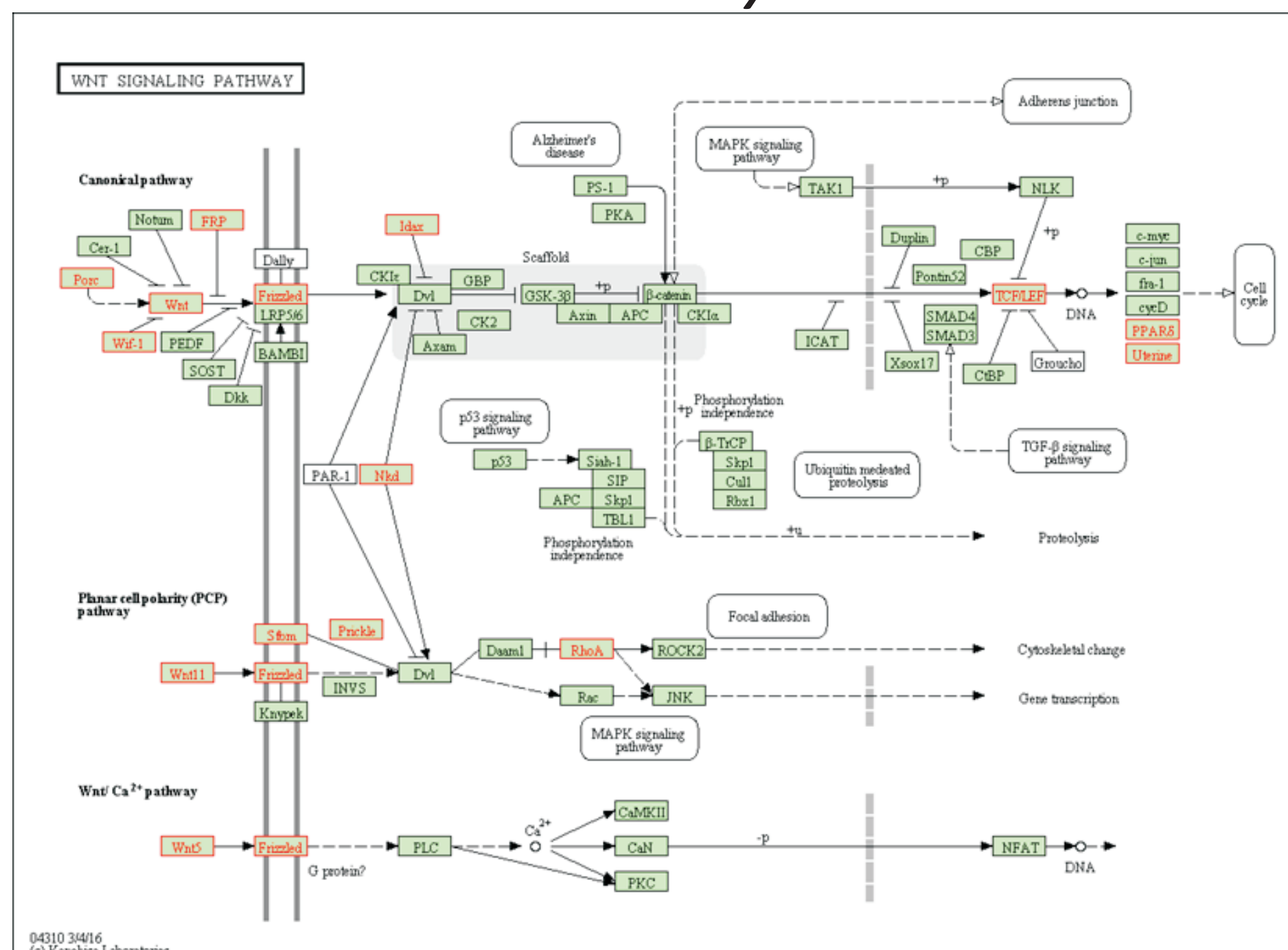


Figure 4: Most of the differentially expressed genes were related to WNT canonical signaling pathway. KEGG representation of WNT signaling pathway. The 26 differentially expressed genes expressed from WNT signaling pathway identified by PCR array are represented in the three WNT signaling pathways with red boxes. Red boxes indicate changes in hMSC-AML gene expression when compared hMSC-HD.

METHODOLOGY

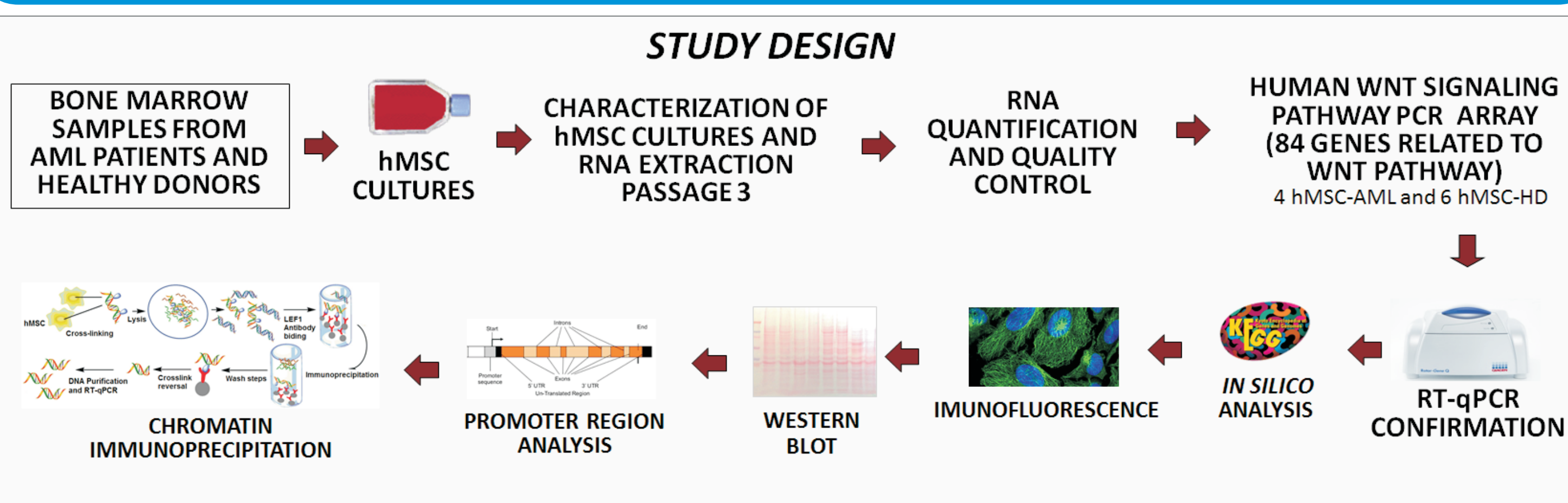


Figure 1: Schematic diagram of the study methodology.

β-CATENIN Immunofluorescence

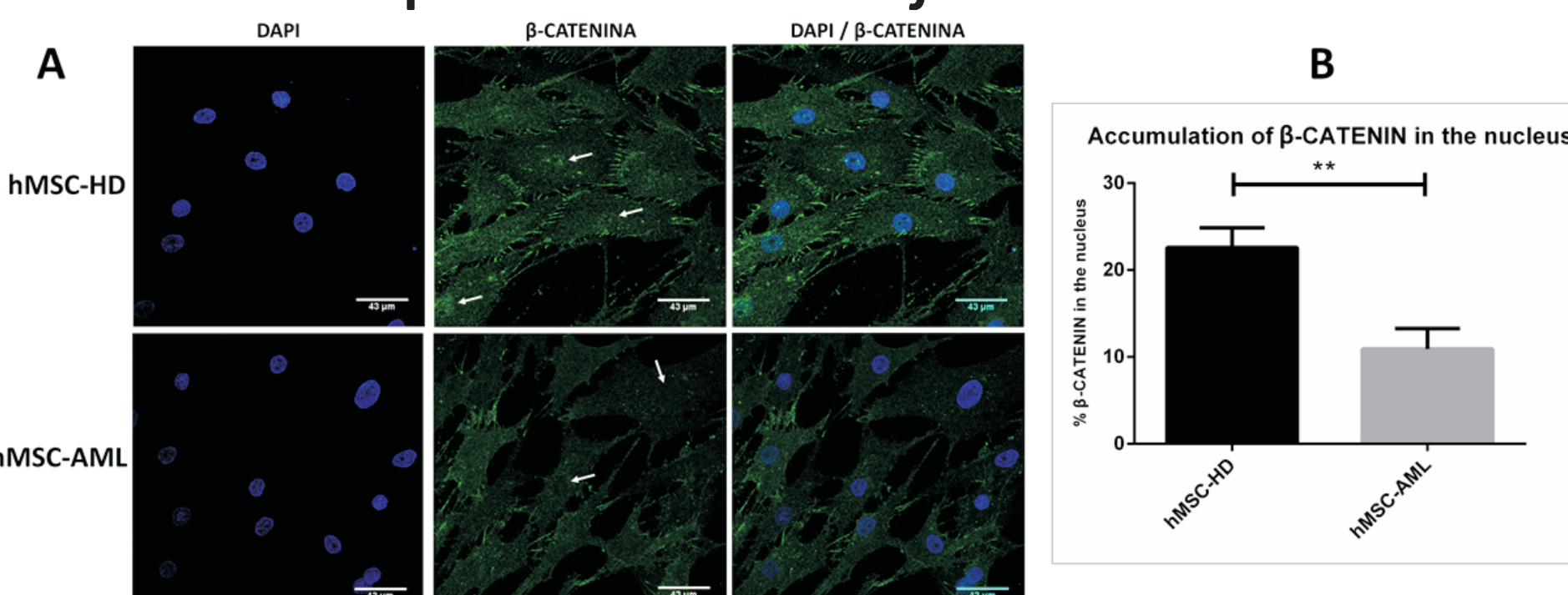


Figure 5: Levels of β-catenin is decreased in hMSC-AML nucleus. (A) Through confocal microscopy we observed the differences in nuclear localization of β-catenin in hMSC-AML (n=5) when compared with hMSC-HD (n=6) obtained in immunofluorescence assays. Nuclei were stained with DAPI (blue) and β-catenin (green-labeled) (63x magnification). (B) Figure representative of nuclear localization of β-catenin in hMSC-AML (n=5) when compared with hMSC-HD (n=6). The bars indicate the localization β-catenin in nucleus (± standard deviation) ** p < 0.01.

LEF1 Western Blot analysis

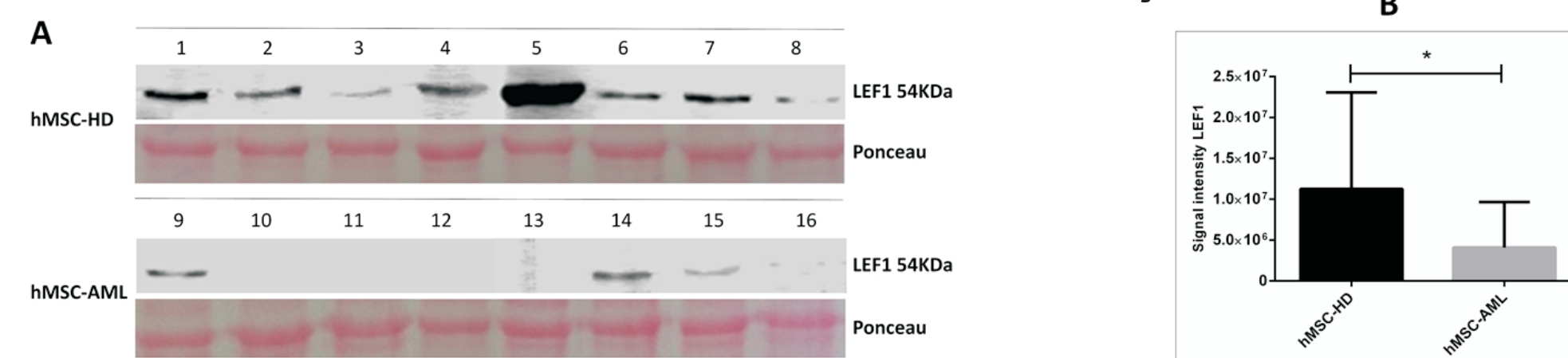


Figure 6: LEF1 protein expression decreased in hMSC-AML. (A) Western blot analysis of LEF1. 30 μg of protein extracts from hMSC-HD (1-8) and hMSC-AML (9-16) were separated on SDS-PAGE and probed with of LEF1 antibody. Ponceau staining was used as a loading control. (B) A representative graphic from the gel results confirmed a decrease of the LEF1 in hMSC-AML when compared to hMSC-HD. The bars indicate the means in protein levels (± standard deviation) * p < 0.05.

β-CATENIN and LEF1 Immunofluorescence

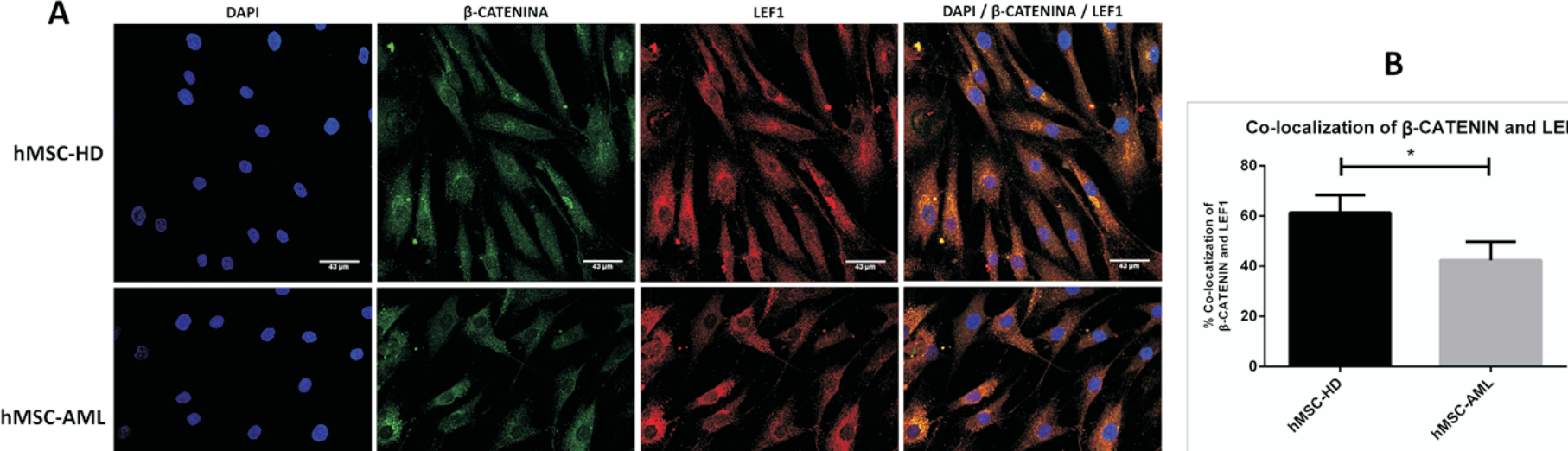


Figure 7: The β-catenin / TCF-LEF complex is decrease in hMSC-AML. (A) Through confocal microscopy we observed the differences in β-catenin / TCF-LEF complex formation in hMSC-AML when compared with hMSC-HD obtained in immunofluorescence assays. Nuclei were stained with DAPI (blue), LEF1 were red-labeled and β-catenin were green-labeled (63x magnification). (B) Figure representative of co-localization of β-catenin and LEF1 in hMSC-AML (n=5) when compared with hMSC-HD (n=6). The bars indicate the co-localization β-catenin and LEF1 (± standard deviation) ** p < 0.01.

BMP4 promoter region analysis

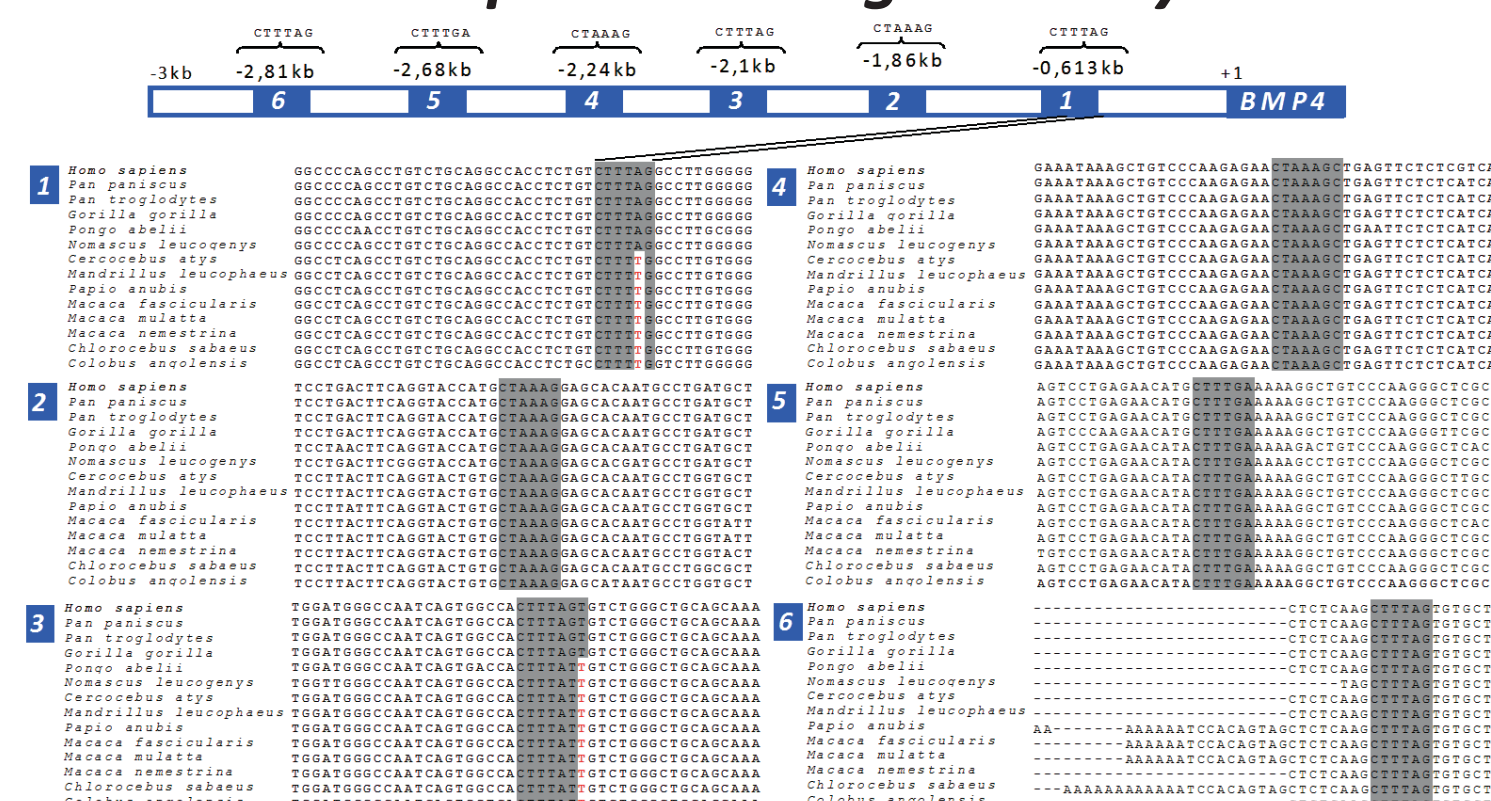


Figure 8: Schematic representation of putative TCF/LEF consensus binding sites in 3kb of *BMP4* gene promoter region predicted manual and by Transfac, Tssitescan, Genomatix and GeneAtlas bioinformatics tools. Six TCF/LEF consensus binding sites were identified in the 3kb of *BMP4* promoter region (5'-CTTGA-3'; 3'-TCAAAG-5' or 5'-CTTAG-3'; 3'-CTAAG-5'). An alignment of the DNA region showed evolutionary conservation among mammals' species. Identical nucleotides are in bold. Gray lines indicate regions investigated by chromatin immunoprecipitation. +1: transcription start site.

Chromatin immunoprecipitation assay

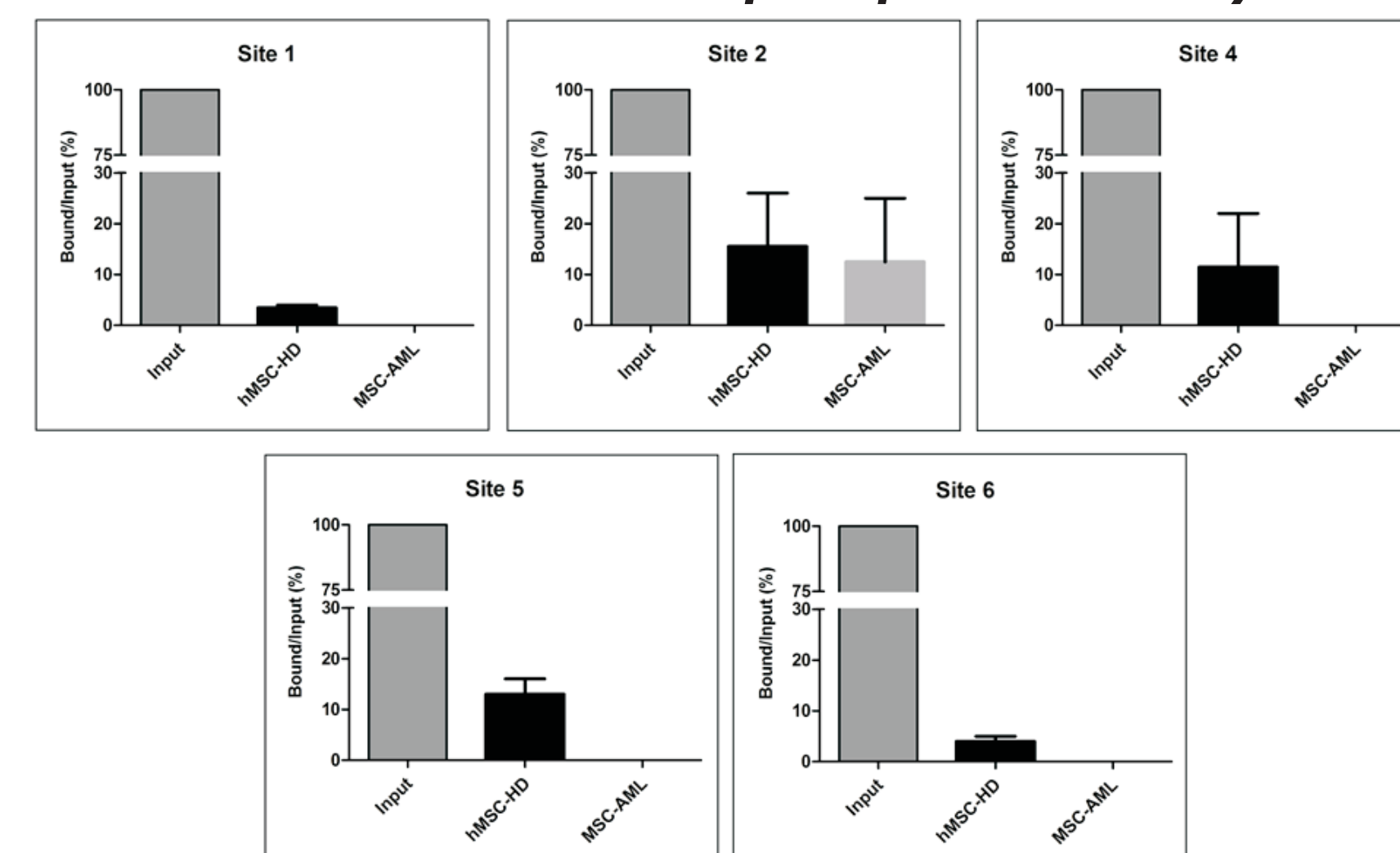


Figure 9: Chromatin immunoprecipitation assay with LEF1 followed by RT-qPCR of predicted TCF/LEF binding sites in the *BMP4* gene promoter. We observed less binding of LEF1 in TCF/LEF consensus binding sites 1, 4, 5, and 6 from hMSC-AML in comparison to hMSC-HD. The histograms set a fold-change of each site by comparing the input control. The data were expressed as the mean ± SD.

CONCLUSION

Altogether, we suggest that the WNT canonical pathway is potentially capable of acting in the regulation of the *BMP4* gene in hMSC-AML

Projeto Gráfico: Setor de Edição e Informação Técnico-Científica / INCA